Molecular Cell, Volume *50*

Supplemental Information

Neurodegeneration-Associated Protein Fragments as Short-Lived Substrates of the N-End Rule Pathway

Christopher S. Brower, Konstantin I. Piatkov, and Alexander Varshavsky

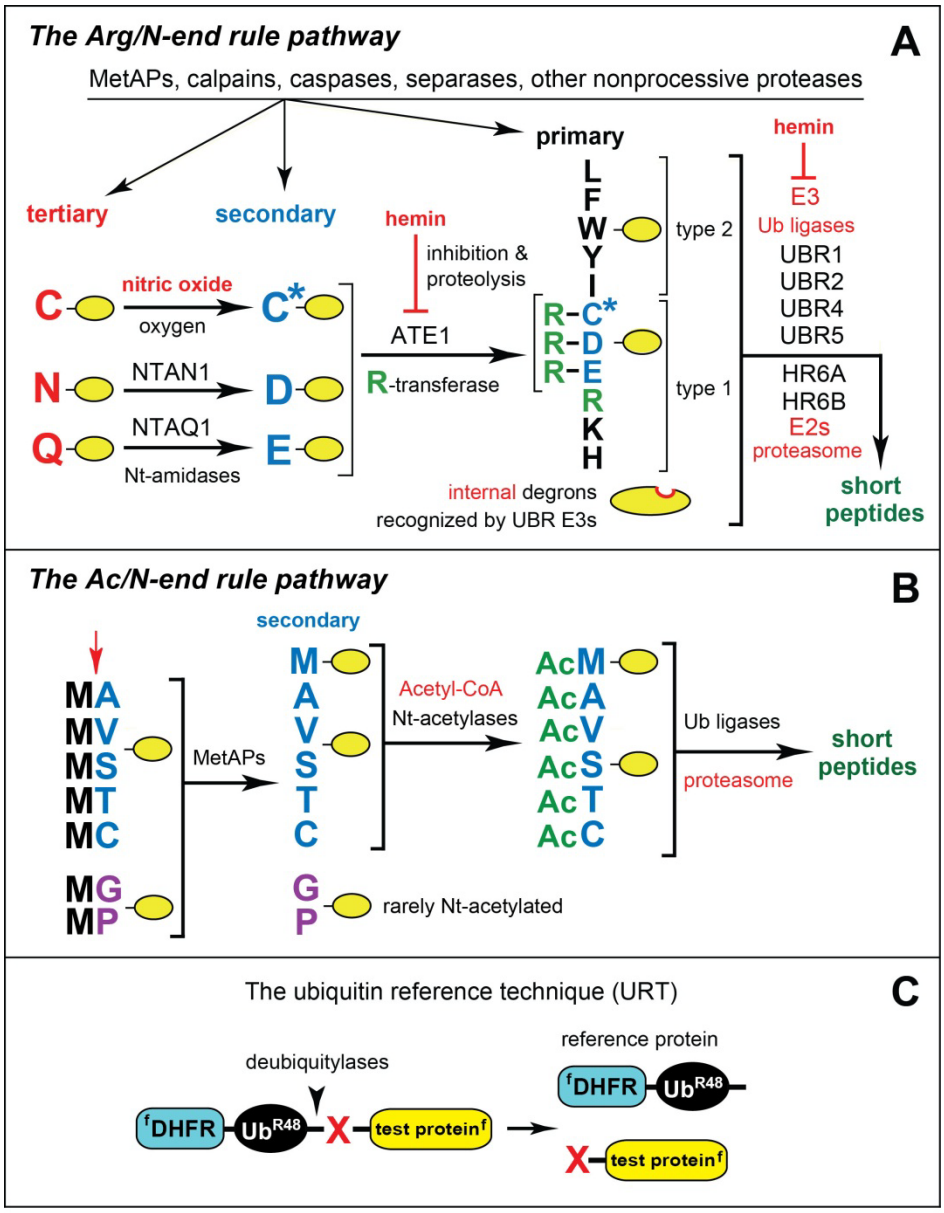

Figure S1, Brower et al.

Figure S1. The mammalian N-end rule pathway. N-terminal residues are indicated by single-letter abbreviations for amino acids. A yellow oval denotes the rest of a protein substrate. E3 ubiquitin (Ub) ligases of the N-end rule pathway are called N-recognins.

(A) The Arg/N-end rule pathway. “Primary”, “secondary” and “tertiary” denote mechanistically distinct subsets of destabilizing N-terminal (Nt) residues. C* denotes oxidized N-terminal Cys, either Cys-sulfinate or Cys-sulfonate, produced *in vivo* by reactions that require nitric oxide (NO) and oxygen. Oxidized N-terminal Cys is N^{α}-terminally arginylated (Nt-arginylated) by *ATE1*-encoded isoforms of arginyl-tRNA-protein transferase (R-transferase), which also arginylates N-terminal Asp (D) and Glu (E). N-terminal Asn (N) and Gln (Q) are deamidated by the *NTAN1*-encoded Nt^{N}-amidase and the *NTAQ1*-encoded Nt^{Q}-amidase,

respectively. In addition to their binding sites that recognize primary destabilizing N-terminal residues, the UBR1, UBR2, UBR4 and UBR5 (EDD) N-recognins contain binding sites for substrates (denoted by a larger oval) with internal (non-N-terminal) degradation signals. Polyubiquitylated Arg/N-end rule substrates are processively destroyed to short peptides by the 26S proteasome. Hemin (Fe^{3+}-heme) binds to R-transferase, inhibits its Nt-arginylation activity and accelerates its *in vivo* degradation. Hemin also binds to UBR-type N-recognins and alters them functionally, in ways that remain to be understood. Regulated degradation of specific proteins by the Arg/N-end rule pathway mediates the sensing of heme, NO, oxygen, and short peptides; the elimination of misfolded proteins; the regulation of DNA repair; the fidelity of chromosome cohesion/segregation; the signaling by G proteins; the control of peptide import; the regulation of apoptosis, meiosis, viral and bacterial infections, fat metabolism, cell migration, actin filaments, cardiovascular development, spermatogenesis, neurogenesis, and memory; and the functioning of adult organs, including the brain, muscle, testis and pancreas ((Brower and Varshavsky, 2009; Caprio et al., 2010; Choi et al., 2010; Dougan and Truscott, 2011; Eisele and Wolf, 2008; Graciet and Wellmer, 2010; Heck et al., 2010; Hu et al., 2008; Hwang et al., 2010a; Hwang et al., 2010b; Hwang et al., 2011; Kurosaka et al., 2010; Matta-Camacho et al., 2010; Mogk et al., 2007; Nillegoda et al., 2010; Piatkov et al., 2012a; Piatkov et al., 2012b; Tasaki et al., 2012; Varshavsky, 2011; Wang et al., 2009; Wang et al., 2011; Zhang et al., 2010), and refs. therein).

(B) The Ac/N-end rule pathway. Although it is virtually certain that this pathway is present in all eukaryotes (Varshavsky, 2011), it has been characterized, thus far , only in *S. cerevisiae* (Hwang et al., 2010b). This diagram illustrates the mammalian Ac/N-end rule pathway through extrapolation from its *S. cerevisiae* version. Red arrow on the left indicates the removal of N-terminal Met by Met-aminopeptidases (MetAPs). N-terminal Met is retained if a residue at position 2 is nonpermissive (too large) for MetAPs. If the retained N-terminal Met or N-terminal Ala, Val, Ser, Thr, and Cys are followed by acetylation-permissive residues, the above N-terminal residues are Nt-acetylated by ribosome-associated Nt-acetylases (Arnesen et al., 2009). The resulting N-degrons are called Ac/N-degrons, to distinguish them from other N-degrons (Hwang et al., 2010b; Varshavsky, 2011). Although the second-position Gly or Pro residues can be made N-terminal by MetAPs , few proteins with N-terminal Gly or Pro are Nt-acetylated (Arnesen et al., 2009). The term “secondary” refers to the Nt-acetylation of a destabilizing N-terminal residue before a protein can be recognized by a cognate N-recognin.

(C) The Ub reference technique (URT), derived from the Ub fusion technique (Piatkov et al., 2012a; Suzuki and Varshavsky, 1999; Varshavsky, 2005). Cotranslational cleavage of a URT-based fusion by deubiquitylases produces, at the initially equimolar ratio, a test protein with a desired N-terminal residue and a “reference” protein such as ^{f}DHFR-Ub^{R48}, a flag-tagged derivative of the mouse dihydrofolate reductase. In URT-based pulse-assays, the labeled test protein is quantified by measuring its level relative to the levels of a stable reference at the same time point. In addition to being more accurate than pulse-chases without a stable reference, URT assays make it possible to detect and measure the degradation of a test protein during the pulse, i.e., before the chase (Piatkov et al., 2012a; Varshavsky, 2005).

Figure S1 refers to Figures 1 and 3.

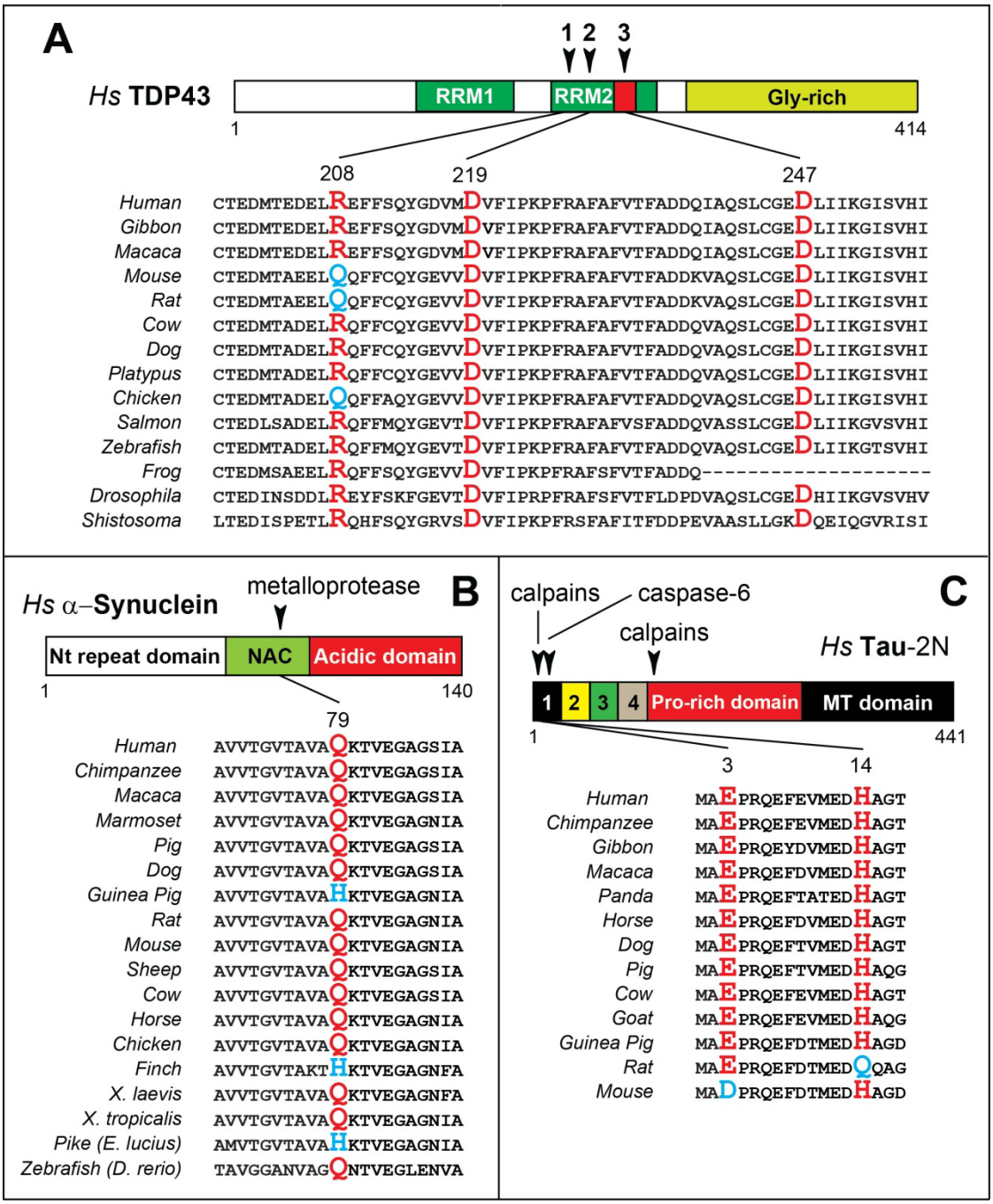

Figure S2, Brower et al.

Figure S2. Evolutionary conservation of the destabilizing nature of P1' residues in the cleavage sites that yield the natural fragments of TDP43, α-Synuclein, and Tau. (A P1' residue becomes N-terminal upon protein cleavage.)

(A) Domain organization of TDP43. Arrowheads indicate the cleavage sites 1, 2 and 3 in full-length TDP43 that yield the natural C-terminal fragments isolated from protein aggregates in human FTLD-TDP brains (see Figure 1 and the main text) (Igaz et al., 2009; Nonaka et al., 2009;

Pesiridis et al., 2011; Wang et al., 2012). The identity of protease(s) that generates these TDP43 fragments is unknown. The indicated residue numbers, including those of P1' residues (these residues are in color and in a lager font size), are of the full-length human TDP43. Note the complete conservation of the P1' Asp (D) residues at the cleavage sites 2 and 3 (positions 219 and 247). Note also the "drift-with-constraint" evolutionary pattern of the P1' residues in the cleavage site 1 (see the main text). Specifically, a P1's residue is Arg (R) in most species but Gln (Q), another destabilizing residue, in the mouse, rat, and chicken.

(B) Domain organization of human α-synuclein. Arrowhead indicates the metalloprotease cleavage site (Choi et al., 2011). (Metalloproteases are usually extracellular but can occur in the cytosol as well (Cauwe and Opdenakker, 2010).) For notations, see A. Analogously to the evolutionary pattern observed with P1' residues in the cleavage site 1 of TDP43 in A, most P1 residues in the cleavage site of α-synuclein are Gln (Q), at position 79 of the human α-synuclein. However, some mammals (such as guinea pigs), some frogs (such as *Xenopus laevis*), and some fishes (such as pikes) contain His at the P1' position of their α-synucleins (Figure S2B). Both N-terminal Gln and His are destabilizing residues (Figure S1A). Yet another informative aspect of evolution of the P1' residue of α-synuclein is that all changes of the predominant Gln at the P1' position (equivalent to position 79 in human α-synuclein) in separate vertebrate lineages (mammals, frogs, fishes) were invariably to His, rather than to another residue. A plausible explanation stems from the fact that the CAA/CAG codons for Gln differ from the CAT/CAC codons for His by one nucleotide. A similar interpretation is also relevant to the evolutionary change of a P1's residue at position 208 in human TDP43 (panel A): the alteration from Arg to Gln at the P1' position of full-length TDP43 in vertebrates involved a single-base transition between the CGG Arg codon and the CAG Gln codon.

(C) Domain organization of the human Tau-2N isoform. Two arrowheads indicate the calpain cleavage sites. In the first of them, the P1' residue of human Tau is Glu (E), at position 3. The third cleavage site is specific for caspases, in particular caspase-6, with the P1' residue being His (H), at position 14 (Spires-Jones et al., 2011; Zilka et al., 2012). In yet another example of the drift-with-constraint evolutionary pattern of P1' residues seen above with TDP43 and α-synuclein (panels A and B), the P1' residue at position 3 of the calpain cleavage site of Tau-2N is Glu in humans, horses, rats, chickens and other vertebrates, but is Asp in mice. Both His, Glu and Asp are destabilizing residues (Figure S1A). Caspases have been shown to cleave human Tau-2N between Asp13 and His14, and also 19 residues upstream of its C-terminus, at Asp421-Ser422, with the former cleavage mediated by at least caspase-6 ((Horowitz et al., 2004) and refs. therein). The Asp13-His14 cleavage produces the N-terminally truncated Tau bearing N-terminal His, a destabilizing residue. The resulting His14-Tau is yet another (predicted) physiological substrate of the Arg/N-end rule pathway. All but one among the examined mammalian Tau sequences has His at the P1' position (this residue becomes N-terminal after caspase cleavage). The only exception, rat Tau, has Gln (Q) at this position, but both His and Gln are destabilizing residues, a recurrent example of the drift-with-constraint pattern of P1' residues described above for other neurodegeneration-associated fragments.

The evolutionary retention of a destabilizing nature of a P1' residue in a precursor of a caspase-generated fragment of any protein (not only of Tau) is noteworthy for an additional and independent reason as well. More than 90% of caspase cleavage sites in cellular proteins contain, at their P1' positions, small residues such as Gly, Ser , Thr and Ala (Crawford and Wells, 2011; Pop and Salvesen, 2009). These residues are not recognized by the Arg/N-end rule pathway (Figure S1A). Thus, remarkably, the destabilizing P1' residues His or Gln in the precursors of

caspase-generated X14-Tau fragments in different mammals (let alone the evolutionary conservation of these residues) would not be expected on a priori grounds, given the major preponderance of smaller P1' residues in caspase substrates at large. Together with our previous findings (Piatkov et al., 2012a; Varshavsky, 2012), these results strongly suggest adaptive (fitness-increasing) origins of the observed destabilizing P1' residues in the precursors of the TDP43, α-synuclein, and Tau fragments examined in the present work.

Figure S2 refers to Figures 1, 2 and 3.

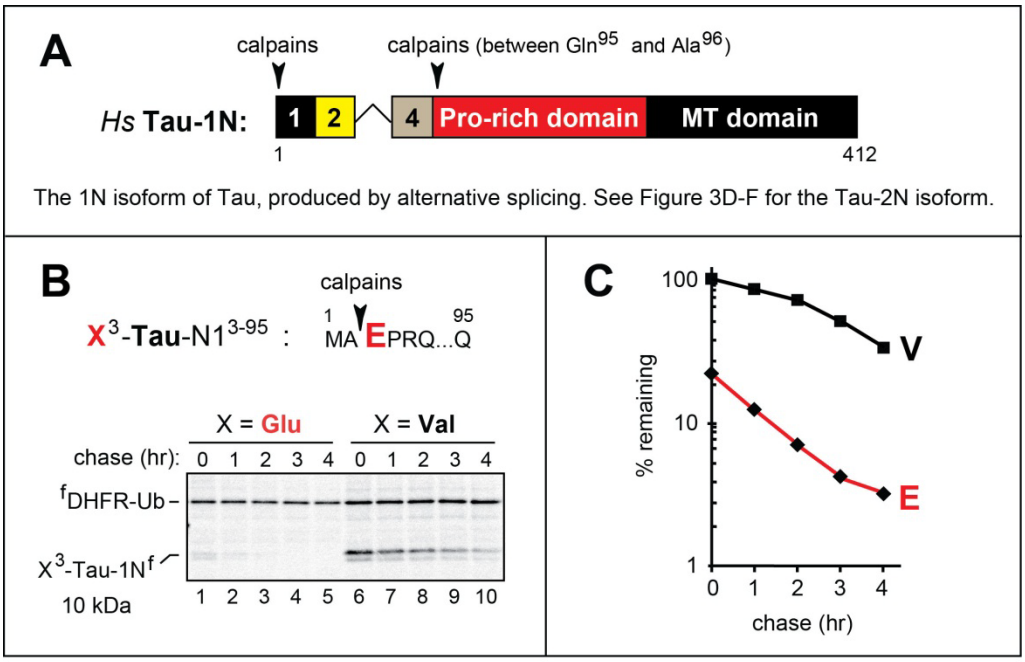

Figure S3, Brower et al.

Figure S3. The Natural C-Terminal Fragment of Human Tau-1N As a Short-Lived Substrate of the Arg/N-End Rule Pathway.

(A) Domain organization of human Tau-1N. Arrowheads indicate the calpain cleavage sites. See also Figure 3D-F and the main text.

(B) The N-terminus-proximal cleavage site is indicated by an arrowhead, with the P1' Glu (E) residue shown in red. The $\mathbf{X}^3$-Tau-1N^{95} fragments, produced from ^{f}DHFR-Ub^{R48}-$\mathbf{X}^3$-Tau-1N^{95} fusions (**X**= Glu, Val) in reticulocyte extract, were assayed for degradation as described in the legend to Figure 1B.

(C) Quantification of B using the reference protein ^{f}DHFR-Ub^{R48}.

Figure S3 refers to Figure 3D, E.

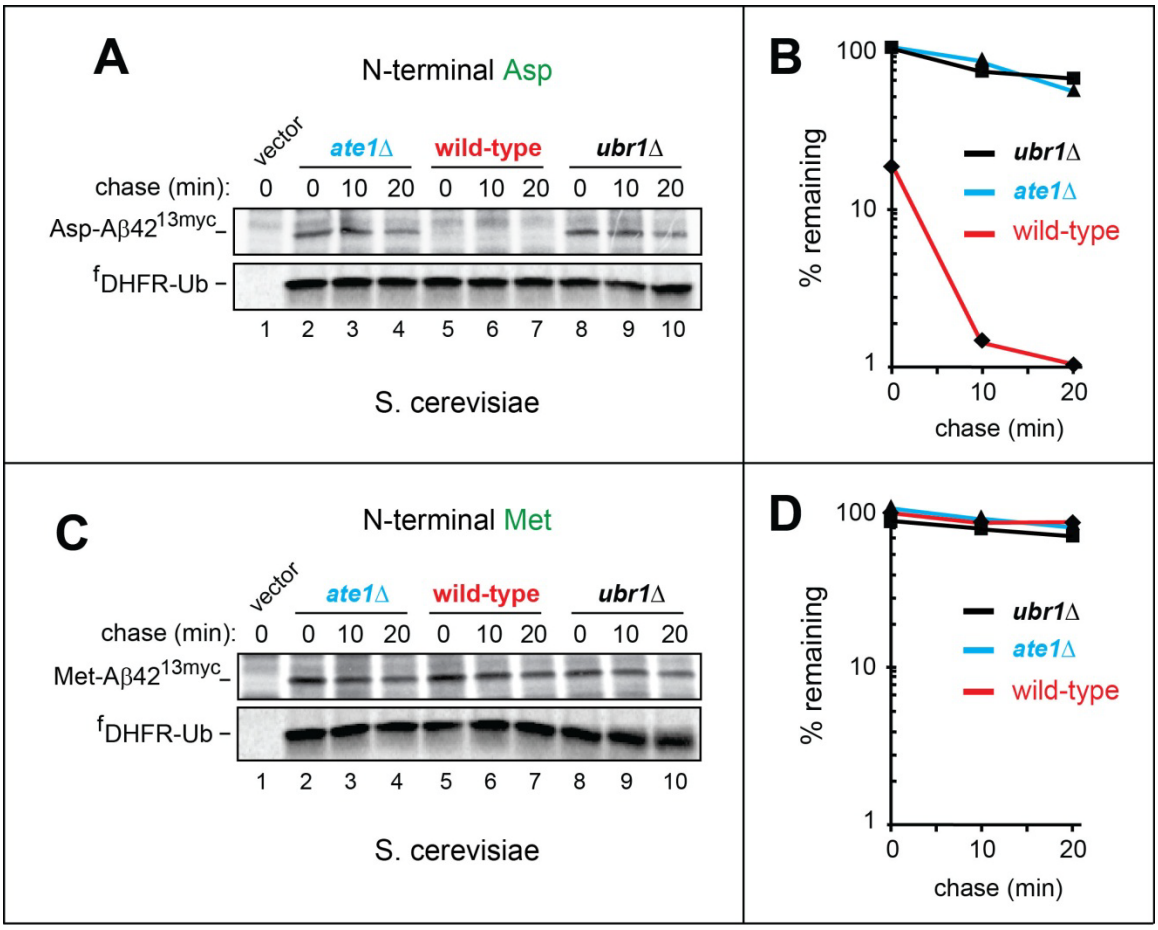

Figure S4, Brower et al.

Figure S4. ^{35}S-Pulse-Chase Assays in *S. cerevisiae* with URT fusions encoding **X**-Aβ42^{13myc}.

(A) The ^{f}DHFR-Ub^{R48}-Asp-Aβ42^{13myc} URT-type fusion, was expressed in wt, *ate1Δ,* or *ubr1Δ S. cerevisiae* as described in Supplemental Experimental Procedures. The fusion's cotranslational cleavage by deubiquitylases produced the reference ^{f}DHFR-Ub^{R48} and the test protein Asp-Aβ42^{13myc}. These proteins were pulse-labeled with ^{35}S-Met/Cys for 5 min at 30°C, followed by the chase for 0, 10 and 20 min, preparation of cell extracts, immunoprecipitation with anti-myc/anti-flag antibodies, SDS-PAGE and autoradiography. Lane 1, *S. cerevisiae* were transformed with vector alone (negative control). Lanes 2-4, Asp-Aβ42^{13myc} and ^{f}DHFR-Ub^{R48} in *ate1Δ* cells lacking Nt-arginylation. Lanes 5-7, same as lanes 2-4 but in wt *S. cerevisiae*. Lanes 8-10, the same as lanes 2-4 but in *ubr1Δ* cells lacking the N-recognin of the Arg/N-end rule pathway. The bands of ^{35}S-labeled Asp-Aβ42^{13myc} and ^{f}DHFR-Ub^{R48} are indicated on the left.

(B) Quantification of A.

(C) Same as in A but ^{f}DHFR-Ub^{R48}-Met-Aβ42^{13myc} whose in vivo cleavage by deubiquitylases yields Met-Aβ42^{13myc}.

(B) Quantification of C.

Figure S4 refers to Figures 4 and 5.

SUPPLEMENTAL EXPERIMENTAL PROCEDURES

Miscellaneous Reagents

Cycloheximide was from Sigma (St. Louis, MO). Human cDNAs encoding proteins examined in the present work were from OpenBiosystems (Huntsville, AL). MG132 (BML-PI102-0005) and clasto-Lactacystin β-Lactone (BML-PI108-0100) were from EnzoLife Sciences (Farmingdale, NY). Epoxomicin (E3652), Thiorphan (T6031), Racecadotil (SML0043), Phosphoramidon (R7385) and Verapamil (V4629) were from Sigma. The following antibodies were used: anti-FLAG M2 (Sigma, F1804), anti-c-Myc (Sigma, C3956), anti-Beta-Amyloid (4G8) (Covance, SIG-39220), anti-Amyloid Precursor Protein (Calbiochem, 171610); and affinity-purified polyclonal antibody to mouse Ate1 (Hu et al., 2005). The following reagents were used for immunoprecipitation: anti-flag M2 Magnetic Beads (Sigma, M8823) and EZview Red anti-c-Myc affinity gel (Sigma, E6654). Detection was carried out using HRP-conjugated goat anti-Rabbit (BioRad, 170-6515) or anti-mouse (BioRad, 170-6516) antibodies and either ECL Prime Western Blotting Detection System (GE Healthcare, UK) or SuperSignal West Femto reagents (Thermo Scientific, Rockford, IL), according to manufacturers' protocols. 5xFAD mice were obtained from The Jackson Laboratories (JAX stock number 006554). Postmortem human brain tissue was obtained from the Harvard Brain Tissue Resource Center.

Plasmids, cDNAs, and Primers

DH5α *E. coli* (Invitrogen) was used for cloning and maintaining plasmids. Phusion High-Fidelity DNA polymerase (New England Biolabs) was used for polymerase chain reaction (PCR). Sequences of all constructed plasmids were verified by DNA sequencing.

Asp-Aβ42^{13myc}. cDNA encoding human Aβ42 sequence (Figure 4A) was amplified by PCR using a set of overlapping forward primers (CB302F, CB268F, CB269F, CB270F, and CB271F) and reverse primers (CB272R, CB273R, CB274R, and CB304R) (Table S2) whose assembled sequence contained DNA encoding human Aβ42. The resulting DNA fragment was inserted into pFA6a-13Myc-kanMX6 (Table S1) using *Sac*II/*Sma*I sites to produce pCB253. The Aβ42^{13myc}-coding sequence was removed from pCB253 using *Sac*II/*Eco*RI and inserted into *Sac*II/*Eco*RI-cut pCH280 (Hwang et al., 2009) to produce pCB255, a low copy plasmid which was used to express ^{f}DHFR-Ub^{R48}-Asp-Aβ42^{13myc} from the P_{MET25} promoter in *S. cerevisiae*. ^{f}DHFR-Ub^{R48}-**X**-Aβ42^{13myc} fusions (**X**=Met, Val, Arg-Asp) were constructed by amplifying the human Aβ42-coding DNA fragment with the following sets of primers: CB313F and CB304R (Met-Aβ42^{13myc}); CB314F and CB304R (Val-Aβ42^{13myc}); CB316F and CB304R (Arg-Asp-Aβ42^{13myc}). The resulting fragments were cut with *Sac*II and *Sma*I, and cloned into *Sac*II/*Sma*I-cut pCB255 to produce the plasmids pCB255, pCB282, pCB284, and pCB285 (Table S1). For ^{35}S-pulse-chase URT-based assays in rabbit reticulocyte extract, the DNA fragment encoding ^{f}DHFR-Ub-Asp-Aβ^{13myc} was removed from pCB255 by *Hind*III digestion and inserted into *Hind*III-cut pcDNA3.0 (Invitrogen) to produce pCB268 (Table S1).

TDP43. The human *Tdp43* cDNA was obtained from OpenBiosystems (ID: LIFESEQ2505218). DNA fragments encoding **X**208-TDP43 C-terminal fragments (**X**=Arg, Met, Gln, and Glu) were constructed by amplification, using the following sets of primers: CB320F and CB327R (Arg208-TDP43); CB321F and CB327R (Met208-TDP43); CB322F and CB327R (Gln208-TDP43); and CB323F and CB327R (Glu208-TDP43) (Table S2). C-terminal flag tags were added by sequential PCR extension using the above forward primers with, at first, CB275R, and then CB280R. The resulting PCR products, which encoded **X**208-TDP43^{f}, were

cut with *Sac*II/*Xba*I and cloned into *Sac*II/*Xba*I-cut pCB268, producing the plasmids pCB322, pCB323, pCB234, and pCB325 (Table S1). DNA encoding **X**219-TDP43^{f} C-terminal fragments (**X**=Asp, Met, Val, and Arg-Asp) were amplified from pCB323 using the following sets of primers: CB330F and CB329R (Asp219-TDP43^{f}); CB331F and CB329R (Met219-TDP43^{f}); CB332F and CB329R (Val219-TDP43^{f}); and CB333F and CB329R (ArgAsp219-TDP43^{f}). DNA encoding X247-TDP43^{f} C-terminal fragments (X=Asp, Met, Val, and Arg-Asp) were amplified from pCB323 using the following sets of primers: CB334F and CB329R (Asp247-TDP43^{f}); CB335F and CB329R (Met247-TDP43^{f}); CB336F and CB329R (Val247-TDP43^{f}); and CB337F and CB329R (Arg-Asp247-TDP43^{f}). The resulting PCR products, which encoded either X219-TDP43^{f} or X247-TDP43^{f}, were cut with *Sac*II/*Xba*I and cloned into *Sac*II/*Xba*I-cut pCB268, producing the plasmids pCB326-pCB333 (Table S1).

For mammalian expression using the weaker (relative to the P_{CMV} promoter) P_{SV40} promoter, DNA fragments encoding the ^{f}DHFR-Ub-**X**-TDP43^{f} fusions in pcDNA3.0-based plasmids (containing the P_{CMV} promoter) were used to replace the luciferase reporter in pGL3-Control plasmid (Promega) after digestion with *Hind*III/*Xba*I.

To construct the plasmid pCB400, used in *in vivo* aggregation assays (Figure 2C-E), DNA encoding mCherry was amplified from pKP551 (Table S1) using primers CB383F and CB384R, and the resulting PCR product was used to replace the ^{f}DHFR moiety in pCB338 after digestion with *Hind*III/*Age*I .

α-Synuclein. The human α-synuclein cDNA was obtained from OpenBiosystems (ID: 5287266). DNA encoding **X**79- αSyn^{f} (X= Gln and Val) were constructed by amplification with the following sets of primers: CB364F and CB367R (Gln79-αSyn); and CB365F and CB367R (Val79-αSyn). The resulting DNA fragments were cut with *Sac*II/*Xba*I, and cloned into *Sac*II/*Xba*I-cut pCB268, generating the plasmids pCB347 and pCB348 (Table S1).

Tau. The human Tau-1N cDNA (lacking exon 3) was obtained from OpenBiosystems (ID: LIFESEQ6770882). DNA encoding **X**^{3}-Tau-1N^{95f} (**X**= Glu and Val) were constructed by amplification with the following sets of primers: CB373F and CB377R (Glu3-TauN1) and CB375F and CB377R (Val3-TauN1). CB377 encoded the C-terminal sequence PGSDYKDDDDK, containing the linker and the flag epitope. Human Tau-2N cDNA (containing exon 3) was obtained by a three-step PCR strategy whereby the N-terminal portion of the Tau$^{3\text{-}124}$-coding fragment was amplified using the above forward primers and CB379R (whose 5'-proximal region is the reverse complement of the 5'-region of CB380F). The C-terminal portion of the Tau$^{3\text{-}124}$-coding fragment was amplified using CB380F (whose 5'-proximal region is the reverse complement of the 5'-region of CB379R) and CB377R. The entire Tau-2N$^{3\text{-}124}$-coding fragment was amplified using the overlapping N- and C-terminal fragments as templates in a final PCR step that employed CB373F and CB377R (Glu3-Tau-2N^{124}) as well as CB375F and CB377R (Val3-Tau-2N^{124}). The resulting DNA fragments were cut with *Sac*II/*Xba*I and cloned into *Sac*II/*Xba*I-cut pCB268, producing the plasmids pCB383, pCB385, pCB386, and pCB388 (Table S1).

In Vitro Transcription-Translation-Degradation Assay

The TNT T7 Coupled Transcription/Translation System, a version of the Promega's rabbit reticulocyte extract preparation in which the main components of the system were supplied separately, was used to carry out transcription-translation-degradation assays. Reaction samples were prepared according to the manufacturer's instructions. Nascent proteins in reticulocyte extract were pulse-labeled with [^{35}S]L-methionine (0.55 mCi/ml, 1,000 Ci/mmol,

MP Biomedicals) for 10 min at 30°C, in the total volume of 30 µl. The labeling was quenched by the addition of cycloheximide and unlabeled methionine, to the final concentrations of 0.1 mg/ml and 5 mM, respectively. Samples were withdrawn at indicated timepoints of a chase and the reactions were terminated by the addition of 0.1 ml of TSD buffer (1% SDS, 5 mM dithiothreitol (DTT), 50 mM Tris-HCl, pH 7.4) and snap-freezing in liquid nitrogen. Samples were then heated at 95°C for 10 min, diluted with 10 volumes of TNN buffer (0.5 % NP-40, 0.25 M NaCl, 5 mM EDTA, 50 mM Tris-HCl, pH 7.4), containing the "complete protease-inhibitor mixture" (Roche), clarified by centrifugation at 20,000*g* for 5 min and immunoprecipitated using 5 µl of beads with an immobilized antibody, either anti-flag M2 Magnetic Beads or EZview Red anti-c-Myc affinity gel. The immunoprecipitates were incubated with rocking at 4°C for 3 hr, followed by 3 washes in TNN buffer, one wash in 10 mM Tris-HCl (pH 8.5), and resuspension in 20 µl of SDS-sample buffer. Samples were then heated at 95°C for 10 min and fractionated by SDS-4-15% PAGE, followed by autoradiography, using Storm PhosphorImager (Molecular Dynamics, Sunnyvale, CA), and quantification, using ImageQuant (GE Healthcare).

Cell Culture

Mouse NIH-3T3 and human HEK-293T cells were obtained from American Type Culture Collection (ATCC, Manassas, VA). *Ate1*$^{-/-}$ mouse embryonic fibroblasts (EFs) were described previously (Kwon et al., 2002). Cells were grown at 37°C in 5% CO_2 in DMEM medium supplemented with 10% fetal bovine serum (FBS) (Gemini Bio-Products, West Sacramento, CA) and penicillin/streptomycin (100 units/ml) (Hyclone). Cells were transfected using Lipofectamine-2000 (Invitrogen) according to the manufacturer's protocol.

In Vivo Degradation Assay

Human embryonic kidney-293T cells (~75% confluent) were transfected with 1 µg plasmid per 35-mm well using Lipofectamine-2000 according to the manufacturer's protocol. Forty hours post-transfection cells were pulse-labeled for 15 min with [^{35}S]L-methionine (0.1 mCi/ml, MP Biomedicals) in DMEM lacking Met and Cys. Labeling was quenched by the addition of cycloheximide (0.1 mg/ml) in complete DMEM (containing Met as well). Cells contained in an entire 35-mm well were lysed at the indicated timepoints of a chase by rapid scraping in 150 µl of TSD buffer (see above) and snap freezing in liquid nitrogen. Samples were then heated at 95°C for 10 min and diluted with 10 volumes of TNN buffer (see above) containing the "complete protease-inhibitor mixture" (Roche). Total ^{35}S (in the 10% CCl_3COOH-insoluble fraction) in samples was then measured, and volumes were adjusted to equalize ^{35}S among different samples. Thus prepared samples were immunoprecipitated by the addition of 5 µl of anti-flag M2 magnetic beads and incubation with rocking at 4°C for 3 hr. Immunoprecipitated proteins were then washed 3 times in TNN buffer and once in 10 mM Tris-HCl (pH 8.5), followed by resuspension in 20 µl of SDS-sample buffer, heating at 95°C for 10 min, SDS-4-15% PAGE, and autoradiography, with quantification as described above.

In Vivo Aggregation Assay

Poly-D-lysine (1 mg/ml)-coated coverslips were placed in 35-mm tissue culture dishes and 1.5×10^5 mouse embryonic fibroblasts (NIH-3T3 or *Ate1*$^{-/-}$) were seeded on top and grown until ~65% confluency. Cells were then transfected with 1 µg of pCB400 per plate, using Lipofectamine-2000. Twenty-four hrs after transfection, cells were fixed in 4% formaldehyde for 10 min at room temperature, and permeabilized in 0.5% Triton-X100 in PBS for 10 min at room

temperature. Coverslips were then washed three times in PBS, and blocked in 10% goat serum for 30 min. Coverslips were incubated with anti-flag M2 antibody (at 1/1000 dilution in 5% goat serum/PBS containing 0.1% Tween-20) for 2 hrs at 37°C in a humid environment, followed by three 5 min washes in PBS containing 0.1% Tween-20 and incubation with fluorescein-conjugated anti-mouse secondary antibody (Pierce, #31567) (at 1/200 dilution in 5% goat serum/PBS containing 0.1% Tween-20) for 1 hr at 37°C in a humid environment. Coverslips were again washed 3 times in PBS containing 0.1% Tween-20, and thereafter were mounted using Vectashield H-1500 mounting medium containing DAPI (Vector Laboratories, Burlingame, CA). Thus processed coverslips were examined for fluorescence by mCherry, DAPI, and fluorescein-conjugated secondary anti-mouse antibody using Zeiss Axio Imager 2.

Steady-State and Pulse-Chase Assays of X-Aβ42^{13myc} in *S. cerevisiae*

S. cerevisiae JD52 (*MATa, trp1-Δ63, ura3–52, his3-Δ200, leu2–3112, lys2-801*) and JD55 (*ubr1Δ::HIS3* in JD52) were described previously(Ghislain et al., 1996). *S. cerevisiae* CHY21 (*ate1Δ::KanMX6* in JD52) and CHY22 (*ubr1Δ::HIS3* in CHY21) were gifts from Dr. Cheol-Sang Hwang. *S. cerevisiae* media included YPD (1% yeast extract, 2% peptone, 2% glucose; only most relevant media components are cited); SD medium (0.17% yeast nitrogen base, 0.5% ammonium sulfate, 2% glucose); and synthetic complete (SC) medium (0.17% yeast nitrogen base, 0.5% ammonium sulfate, 2% glucose, plus a drop-out mixture of compounds required by auxotrophic strains). *S. cerevisiae* were transformed with the low copy pCB255, pCB282, pCB284, or pCB285 plasmids using standard techniques (Ausubel et al., 2010). Expression of ^{f}DHFR-Ub-**X**-Aβ^{13myc} was induced by growth in SD(-Ura, -Met) for 6 hr at 30°C.

^{35}S-pulse-chase experiments with *S. cerevisiae* were performed essentially as described previously (Hwang et al., 2009). Transformed yeast strains carrying low copy plasmids expressing test protein fusions were grown in 10 ml of SD(-Ura) medium at 30°C until A_{600} of ~1.0. Cells were pelleted by centrifugation at 3,000*g* for 10 min and washed with 0.8 ml of fresh pre-warmed medium. Cell pellets were gently resuspended in 0.4 ml of the same medium but lacking Met/Cys, and incubated for 10 min at 30°C, followed by labeling for 5 min with [^{35}S]L-methionine (0.55 mCi/ml, 1,000 Ci/mmol; MP Biomedicals). Cells were then pelleted by centrifugation and resuspended in 0.4 ml of YPD medium containing cycloheximide at 0.1 mg/ml (chase medium). Samples (0.1 ml) were taken at the indicated time points and added to 0.8 ml of the lysis buffer (1% TritonX-100, 0.15 M NaCl, 5 mM EDTA, 1 mM PMSF (phenylmethylsulfonyl fluoride, freshly dissolved), 50 mM HEPES, pH 7.5) containing "yeast protease inhibitor cocktail" (Roche), followed by rapid freezing in liquid nitrogen. Samples were thawed in thermomixer (Eppendorf) at 37°C for 2 min and thereafter treated by 4 runs in lysing matrix C (0.1 mM silica spheres) using FastPrep-24 (MP Biomedicals) (setting 6.5 m/s, 20 sec, with 2 min on ice between the runs). The resulting samples were centrifuged at 20,000*g*, and total ^{35}S (in the 10% CCl_3COOH-insoluble fraction) in each sample was adjusted, by dilution with lysis buffer, to equalize ^{35}S among different samples. Thus prepared samples were immunoprecipitated using EZview Red anti-cMyc affinity gel. The unbound material was immunoprecipitated using anti-flag M2 magnetic beads. Immunoprecipitated proteins were fractionated by SDS-4-15% PAGE, electrophoretically transferred to PVDF membranes, detected by autoradiography, and quantified, using Storm PhosphorImager and ImageQuant.

Animal Care and Treatments

All animal care and procedures were carried out according to the NIH guidelines, and were approved by the Institutional Animal Care and Use Committee and the Office of Laboratory Animal Research (OLAR) at the California Institute of Technology. Mice were housed at ~22°C using a 12 hr light/12 hr dark cycle, with Laboratory Rodent Diet 5001 (PMI International, Richmond, IN) ad libitum. The proteasome inhibitors MG132 (25 μmol/kg) clasto-lactacystin β-lactone (1 μmol/kg), and epoxomicin (0.6 μmol/kg), as well as neprilysin inhibitors Thiorphan (12 mg/kg), Racecadotil (18 mg/kg), and Phosphoramidon (2.5 mg/kg), in addition to verapamil (45 mg/kg), an inhibitor of multidrug resistance transporters, were delivered intraperitoneally (two injections, 12 hrs apart). Twelve hours after the last injection, mouse brains were harvested and proteins were extracted as described below.

Tissue Extracts and Immunoblotting

Proteins were extracted from mouse and human brain samples using a three-step sequential procedure. First, brain tissue (225 mg per ml of buffer) was homogenized in TBS buffer (0.15 M NaCl, 50 mM Tris-HCl, pH7.4) containing "complete protease-inhibitor mixture" (Roche), using FastPrep-24 and Lysing Matrix D (MP Biomedicals), with 3 runs at 6.5 m/s for 30 sec each, and with 5-min incubations on ice between runs. TBS-insoluble material was pelleted by centrifugation at 100,000g for 40 min at 4°C in the TL-100.3 ultracentrifuge. The pellets were washed in TBS, and resuspended in TBS-X (TBS containing 1% Triton-X100) by rotation at 4°C for 30 min TBS-X-insoluble material was precipitated by centrifugation at 100,000g for 40 min at 4°C, washed in TBS, and resuspended in 70% HCOOH (formic acid (FA)), using multiple passages through a 26 gauge needle and overnight rotation 4°C. Material insoluble in 70% HCOOH was pelleted by centrifugation at 22,000*g* for 10 min at 4°C. Protein concentrations in TBS, TBS-X, and FA extracts were determined using Bio-Rad Protein Assay DyeReagent (BioRad, # 500-0006). HCOOH extracts were additionally dried in a Speed-Vac and washed with acetone. Equal total protein amounts from each sample were fractionated by SDS-16.5% PAGE (Criterion Tris-Tricine gels; BioRad, #345-0063), and proteins were transferred to 0.2 μm nitrocellulose membranes (BioRad, # 162-0112), which were then autoclaved in H_2O to enhance epitope exposure to antibodies (Swerdlow et al., 1986), followed by immunoblotting with the specified antibodies. Detection was carried out using ECL Prime Western blotting Detection System (GE Healthcare, UK) or SuperSignal West Fempto reagents (Thermo Scientific, Rockford, IL) according to manufacturer's protocol.

In Vitro Arginylation Assay

In vitro Ate1 arginyl-transferase (R-transferase) assays were carried out in 50-μl samples largely as described previously (Hu et al., 2006). The samples contained either zero, 0.1, or 1.0 μg of purified recombinant Ate1-1, Ate1-2, Ate1-3, or Ate1-4 mouse transferase (Hu et al., 2006) (Hu et al., 2005) and 0.5 mg/ml of chemically synthesized Aβ42 (Sigma, A9810), total *E. coli* tRNA (0.6 mg/ml) (Sigma), total *E. coli* aminoacyl-tRNA synthetases (800 U/ml) (Sigma), 1 mM ATP, 30 mM KCl, 2 mM $MgCl_2$, 2 mM β-mercaptoethanol, 2 μM L-arginine, 10 mM Tris-HCl (pH 8.0) and 0.1 μM [^{14}C]L-arginine (PerkinElmer, NEN Radiochemicals, Waltham, MA). A reaction mixture (50 μl) was incubated for 30 min at 37°C, followed by the addition of the equal volume of 2xSDS sample buffer. Samples were then heated at 95°C for 10 min, followed by SDS-16.5% PAGE (Criterion Tris-Tricine gels; BioRad, #345-0063), electrophoretic transfer to 0.2 μm PVDF membranes using the iBlot apparatus (Invitrogen), and both autoradiography and immunoblotting, as described in the legend to Figure 4D.

Antibody Specific for Arg-Asp-Aβ

Rabbit peptide-mediated antibody to **R**DAEFRHDSGYC, the Nt-arginylated N-terminal sequence of Aβ42 (except for C-terminal Cys, which was used to conjugate the peptide to keyhole limpet hemocyanin, a carrier protein) was produced by Abgent (San Diego, CA), using standard methods. The peptides **R**DAEFRHDSGYC and its "non-arginylated" counterpart DAEFRHDSGYC were synthesized and purified also by Abgent. The resulting antibody (its IgG fraction, produced using immobilized Protein A) was affinity-purified, "positively" at first, against the immobilized **R**DAEFRHDSGYC peptide. The peptide-bound antibody was eluted and thereafter "negatively" purified against the DAEFRHDSGYC peptide (immobilized using SulfoLink Coupling Resin (Pierce)), with collection, this time, of the unbound antibody fraction. The resulting antibody was characterized as described in Figure 5A and the main text, and was then used to detect Nt-arginylated Arg-Asp-Aβ42. Immunoblotting was carried out (with the antibody at 1 μg/ml) overnight at 4°C in 5% skim milk in TBS-T (TBS containing 0.1% Tween-20). Goat anti-rabbit secondary antibody conjugated to horseradish peroxidase was used at 1:2,000 dilution, and detection was performed using one of the two above-described chemilumenescence systems.

Table S1. Plasmids used in this study.

Plasmid	Description	Source or Reference
pcDNA3.0-Neo	Amp^R; Neo^R; Expression vector for cloning your gene of interest	Invitrogen
pGL3-Control	Amp^R; luciferase reporter driven by SV40 promoter. Also contains the SV40 enhancer.	Promega
pAF6a-13myc-kanMX6	Amp^R; Kan^R; Yeast genomic targeting	Addgene
pCH280	Amp^R; pRS416MET25-^{f}DHFR-Ub^{K48R}-$MGT1^f$	(Hwang et al., 2009)
pKP551	Amp^R; Trp, pBAM- Ub^{K48R}-V-eK-mCherry-Flag-Myc.	This study
IMAGE clone: 5287266	Amp^R; 3' full length human α-synuclein cDNA	Open Biosystems
Clone: LIFESEQ2505218	Amp^R; full length human TDP43 cDNA	Open Biosystems
Clone: LIFESEQ6770882	Amp^R; 5' portion of human Tau-1N cDNA (lacking exon 3)	Open Biosystems
pCB253	Amp^R; Kan^R; pAF6a-13myc-kanMX6 containing Aβ42-13myc tag	This study
pCB255	Amp^R; pRS416MET25-^{f}DHFR-Ub^{K48R}-Aβ42 ^{13myc}	This study
pCB268	Amp^R; Neo^R; pcDNA3.0-based plasmid encoding ^{f}DHFR-Ub^{K48R}-Aβ42 ^{13myc} under the control of T7 or CMV promoter	This study
pCB282	Amp^R; pRS416MET25-^{f}DHFR-Ub^{K48R}-Val-Aβ42 ^{13myc}	This study
pCB284	Amp^R; pRS416MET25-^{f}DHFR-Ub^{K48R}-Arg-Asp-Aβ42 ^{13myc}	This study
pCB285	Amp^R; pRS416MET25-^{f}DHFR-Ub^{K48R}-Met-Aβ42 ^{13myc}	This study
pCB322	Amp^R; Neo^R; pcDNA3.0-based plasmid encoding ^{f}DHFR-Ub^{K48R}-Arg208-$TDP43^f$ under the control of T7 or CMV promoter	This study
pCB323	Amp^R; Neo^R; pcDNA3.0-based plasmid	This study

	encoding ^{f}DHFR-Ub^{K48R}-Met208-TDP43^{f} under the control of T7 or CMV promoter	
pCB324	Amp^{R}; Neo^{R}; pcDNA3.0-based plasmid encoding ^{f}DHFR-Ub^{K48R}-Gln208-TDP43^{f} under the control of T7 or CMV promoter	This study
pCB325	Amp^{R}; Neo^{R}; pcDNA3.0-based plasmid encoding ^{f}DHFR-Ub^{K48R}- Glu208-TDP43^{f} under the control of T7 or CMV promoter	This study
pCB326	Amp^{R}; Neo^{R}; pcDNA3.0-based plasmid encoding ^{f}DHFR-Ub^{K48R}-Asp219-TDP43^{f} under the control of T7 or CMV promoter	This study
pCB327	Amp^{R}; Neo^{R}; pcDNA3.0-based plasmid encoding ^{f}DHFR-Ub^{K48R}-Met219-TDP43^{f} under the control of T7 or CMV promoter	This study
pCB328	Amp^{R}; Neo^{R}; pcDNA3.0-based plasmid encoding ^{f}DHFR-Ub^{K48R}-Val219-TDP43^{f} under the control of T7 or CMV promoter	This study
pCB329	Amp^{R}; Neo^{R}; pcDNA3.0-based plasmid encoding ^{f}DHFR-Ub^{K48R}-ArgAsp219-TDP43^{f} under the control of T7 or CMV promoter	This study
pCB330	Amp^{R}; Neo^{R}; pcDNA3.0-based plasmid encoding ^{f}DHFR-Ub^{K48R}-Asp247-TDP43^{f} under the control of T7 or CMV promoter	This study
pCB331	Amp^{R}; Neo^{R}; pcDNA3.0-based plasmid encoding ^{f}DHFR-Ub^{K48R}-Met247-TDP43^{f} under the control of T7 or CMV promoter	This study
pCB332	Amp^{R}; Neo^{R}; pcDNA3.0-based plasmid encoding ^{f}DHFR-Ub^{K48R}-Val247-TDP43^{f} under the control of T7 or CMV promoter	This study
pCB333	Amp^{R}; Neo^{R}; pcDNA3.0-based plasmid encoding ^{f}DHFR-Ub^{K48R}-ArgAsp247-TDP43^{f} under the control of T7 or CMV promoter	This study
pCB334	Amp^{R}; pGL3-Control-based plasmid encoding ^{f}DHFR-Ub^{K48R}-Asp219-TDP43^{f} under the control of SV40 promoter	This study

pCB336	Amp^R; pGL3-Control-based plasmid encoding ^{f}DHFR-Ub^{K48R}-Val219-TDP43^f under the control of SV40 promoter	This study
pCB338	Amp^R; pGL3-Control-based plasmid encoding ^{f}DHFR-Ub^{K48R}-Asp247-TDP43^f under the control of SV40 promoter	This study
pCB340	Amp^R; pGL3-Control-based plasmid encoding ^{f}DHFR-Ub^{K48R}-Val247-TDP43^f under the control of SV40 promoter	This study
pCB341	Amp^R; pGL3-Control-based plasmid encoding ^{f}DHFR-Ub^{K48R}-ArgAsp247-TDP43^f under the control of SV40 promoter.	This study
pCB347	Amp^R; Neo^R; pcDNA3.0-based plasmid encoding ^{f}DHFR-Ub^{K48R}-Gln79-αSyn^f under the control of T7 or CMV promoter	This study
pCB348	Amp^R; Neo^R; pcDNA3.0-based plasmid encoding ^{f}DHFR-Ub^{K48R}-Val79-αSyn^f under the control of T7 or CMV promoter	This study
pCB383	Amp^R; Neo^R; pcDNA3.0-based plasmid encoding ^{f}DHFR-Ub^{K48R}-Glu3-Tau-2N$^{3\text{-}124f}$ under the control of T7 or CMV promoter	This study
pCB385	Amp^R; Neo^R; pcDNA3.0-based plasmid encoding ^{f}DHFR-Ub^{K48R}-Val3-Tau-2N$^{3\text{-}124f}$ under the control of T7 or CMV promoter	This study
pCB386	Amp^R; Neo^R; pcDNA3.0-based plasmid encoding ^{f}DHFR-Ub^{K48R}-Glu3-Tau-1N^{95f} under the control of T7 or CMV promoter	This study
pCB388	Amp^R; Neo^R; pcDNA3.0-based plasmid encoding ^{f}DHFR-Ub^{K48R}-Val3-Tau-1N^{95f} under the control of T7 or CMV promoter	This study
pCB400	Amp^R; pGL3-Control-based plasmid encoding mCherry-Ub^{K48R}-Asp247-TDP43^f under the control of SV40 promoter	This study

Table S2. PCR Primers used in this study

Primer	Primer's sequence (5' to 3')
CB268	ATATGAGGTTCATCATCAAAAATTGGTGTTCTTTGCTGAA
CB269	GATGTGGGTTCAAACAAAGGTGCGATCATTGGACTCATGG
CB270	TGGGCGGTGTTGTCATAGCGTCTGGTTCCGACTACAAGGA
CB271	CGATGATGACAAGTAAGAATTCGATC
CB272	TTTGATGATGAACCTCATATCCAGAATCATGTCGGAACTC
CB273	CCTTTGTTTGAACCCACATCTTCAGCAAAGAACACCAATT
CB274	CGCTATGACAACACCGCCCACCATGAGTCCAATGATCGCA
CB275	GATCGAATTCTTACTTGTCATCATCGTCCTTGTAGTCGGAACCA GA
CB280	GATCGGGCCCTCTAGATCACTTGTCATCGTCGTCCTTG
CB302	GATCGGATCCCCGCGG TGGTGATGCGGAG
CB304	GATCCCCGGGCGCTATGACAACACCGCCCACC
CB313	GATCCGCGGTGGTATGGCAGAGTTCCGACATGATTCTGGATATG
CB314	GATCCGCGGTGGTGTAGCAGAGTTCCGACATGATTCTGGATATG
CB316	GTTCCGCGGTGGTAGGGATGCAGAGTTCCGACATGATTCTGGAT ATG
CB320	GAATCCGCGGTGGTAGGGAGTTCTTCTCTCAGTACGGGG
CB321	GAATCCGCGGTGGTATGGAGTTCTTCTCTCAGTACGGGG
CB322	GAATCCGCGGTGGTCAGGAGTTCTTCTCTCAGTACGGGG
CB323	GAATCCGCGGTGGTGAAGAATTCTTCTCTCAGTACGGGG
CB327	GTCCTTGTAGTCGGATCCAGACATTCCCCAGCCAGAAGACTT
CB329	AATAGGGCCCTCTAGATCACTTGTCATCGTC
CB330	GAATCCGCGGTGGTGATGTCTTCATCCCCAAGCCATTCAGGGCC
CB331	GAATCCGCGGTGGTATGGTCTTCATCCCCAAGCCATTCAGGGCC
CB332	GAATCCGCGGTGGTGTGGTCTTCATCCCCAAGCCATTCAGGGCC
CB333	GAATCCGCGGTGGTAGAGATGTCTTCATCCCCAAGCCATTCAGG GCC
CB334	GAATCCGCGGTGGTGACTTGATCATTAAAGGAATCAGCGTTC
CB335	GAATCCGCGGTGGTATGTTGATCATTAAAGGAATCAGCGTTC
CB336	GAATCCGCGGTGGTGTGTTGATCATTAAAGGAATCAGCGTTC
CB337	GAATCCGCGGTGGTAGAGACTTGATCATTAAAGGAATCAGCGT TC
CB364	GAATCCGCGGTGGTCAGAAGACAGTGGAGGGAGCAGGG

CB365	GAATCCGCGGTGGTGTGAAGACAGTGGAGGGAGCAGGG
CB367	GAATCCCGGGGGCTTCAGGTTCGTAGTCTTG
CB373	GAATCCGCGGTGGTGAGCCAAGACAGGAGTTCGAAGTGATGGAAG
CB375	GAATCCGCGGTGGTGTGCCAAGACAGGAGTTCGAAGTGATGGAAG
CB377	GATCTCTAGATTACTTGTCATCGTCATCCTTGTAGTCAGACCCGGGTTGGGTCACGTGACCAGCAGC
CB379	GGGGCTGCGCGGCAGCCTGCTTGCCGGGAGCTCCCTCATCCACTAAGGGTGCTGTCACATCTTCCGCTGTTGGAGTGCTC
CB380	GCTCCCGGCAAGCAGGCTGCCGCGCAGCCCCACACGGAGATCCCAGAAGGAACCACAGCTGAAGAAGCAGGCATTGGAG
CB383	GATCAAGCTTCCCACCATGGTGAGCAAGGGCGAGGAGG
CB384	GATCACCGGTCAGAGTCTTGACGAAAATCTGCATGGTCGACCCACTCTTGTACAGCTCGTCCATGCC

SUPPLEMENTAL REFERENCES

Arnesen, T., Van Damme, P., Polevoda, B., Helsens, K., Evjenth, R., Colaert, N., Varhaug, J.E., Vandekerckhove, J., Lillehaug, J.R., Sherman, F., *et al.* (2009). Proteomics analyses reveal the evolutionary conservation and divergence of N-terminal acetyltransferases from yeast to humans. Proc Natl Acad Sci USA *106*, 8157-8162.

Ausubel, F.M., Brent, R., Kingston, R.E., Moore, D.D., Smith, J.A., Seidman, J.G., and Struhl, K. (2010). Current Protocols in Molecular Biology. (New York: Wiley-Interscience).

Brower, C.S., and Varshavsky, A. (2009). Ablation of arginylation in the mouse N-end rule pathway: loss of fat, higher metabolic rate, damaged spermatogenesis, and neurological perturbations. PLoS ONE *4*, e7757.

Caprio, M.A., Sambrooks, C.L., Durand, E.S., and Hallak, M. (2010). The arginylation-dependent association of calreticulin with stress granules is regulated by calcium. Biochem J *429*, 63-72.

Cauwe, B., and Opdenakker, G. (2010). Intracellular substrate cleavage: a novel dimension in the biochemistry, biology and pathology of matrix metalloproteinases. Crit Rev Biochem Mol Biol *45*, 351-423.

Choi, D.H., Kim, Y.J., Kim, Y.G., Joh, T.H., Beal, M.F., and Kim, Y.S. (2011). Role of matrix metalloproteinase 3-mediated alpha-synuclein cleavage in dopaminergic cell death. J Biol Chem *286*, 14168-14177.

Choi, W.S., Jeong, B.-C., Joo, Y.J., Lee, M.-R., Kim, J., Eck, M.J., and Song, H.K. (2010). Structural basis for the recognition of N-end rule substrates by the UBR box of ubiquitin ligases. Nat Struct Mol Biol *17*, 1175-1181.

Crawford, E.D., and Wells, J.A. (2011). Caspase substrates and cellular remodeling. Annu Rev Biochem *80*, 1055-1087.

Dougan, D.A.M., D., and Truscott, K.N. (2011). The N-end rule pathway: from recognition by N-recognins to destruction by AAA+ proteases. Biochim Biophys Acta *1823*, 83-91.

Eisele, F., and Wolf, D.H. (2008). Degradation of misfolded proteins in the cytoplasm by the ubiquitin ligase Ubr1. FEBS Lett *582*, 4143-4146.

Ghislain, M., Dohmen, R.J., Levy, F., and Varshavsky, A. (1996). Cdc48p interacts with Ufd3p, a WD repeat protein required for ubiquitin-mediated proteolysis in Saccharomyces cerevisiae. EMBO J *15*, 4884-4899.

Graciet, E., and Wellmer, F. (2010). The plant N-end rule pathway: structure and functions. Trends Plant Sci *15*, 447-453.

Heck, J.W., Cheung, S.K., and Hampton, R.Y. (2010). Cytoplasmic protein quality control degradation mediated by parallel actions of the E3 ubiquitin ligases Ubr1 and San1. Proc Natl Acad Sci USA *107*, 1106-1111.

Horowitz, P.M., Patterson, K.R., A.L., G.-B., Reynolds, M.R., Carroll, C.A., Weintraub, S.T., Bennett, D.A., Cryns, V.L., Berry, R.W., and Binder, L.I. (2004). Early N-terminal changes and caspase-6 cleavage of tau in Alzheimer's disease. J Neurosci *24*, 7895-7902.

Hu, R.-G., Brower, C.S., Wang, H., Davydov, I.V., Sheng, J., Zhou, J., Kwon, Y.T., and Varshavsky, A. (2006). Arginyl-transferase, its specificity, putative substrates, bidirectional promoter, and splicing-derived isoforms. J Biol Chem *281*, 32559-32573.

Hu, R.-G., Sheng, J., Xin, Q., Xu, Z., Takahashi, T.T., and Varshavsky, A. (2005). The N-end rule pathway as a nitric oxide sensor controlling the levels of multiple regulators. Nature *437*, 981-986.

Hu, R.-G., Wang, H., Xia, Z., and Varshavsky, A. (2008). The N-end rule pathway is a sensor of heme. Proc Natl Acad Sci USA *105*, 76-81.

Hwang, C.-S., Shemorry, A., and Varshavsky, A. (2009). Two proteolytic pathways regulate DNA repair by co-targeting the Mgt1 alkylguanine transferase. Proc Natl Acad Sci USA *106*, 2142-2147.

Hwang, C.-S., Shemorry, A., and Varshavsky, A. (2010a). The N-end rule pathway is mediated by a complex of the RING-type Ubr1 and HECT-type Ufd4 ubiquitin ligases. Nat Cell Biol *12*, 1177-1185.

Hwang, C.-S., Shemorry, A., and Varshavsky, A. (2010b). N-terminal acetylation of cellular proteins creates specific degradation signals. Science *327*, 973-977.

Hwang, C.-S., Sukalo, M., Batygin, O., Addor, M.C., Brunner, H., Aytes, A.P., Mayerle, J., Song, H.K., Varshavsky, A., and Zenker, M. (2011). Ubiquitin ligases of the N-end rule pathway: assessment of mutations in UBR1 that cause the Johanson-Blizzard syndrome. PLoS One *6*, e24925.

Igaz, L.M., Kwong, L.K., Chen-Plotkin, A., Winton, M.J., Unger, T.L., Xu, Y., Neumann, M., Trojanowski, J.Q., and Lee, V.M. (2009). Expression of TDP-43 C-terminal fragments in vitro recapitulates pathological features of TDP-43 proteinopathies. J Biol Chem *284*, 8516-8524.

Kurosaka, S., Leu, N.A., Zhang, F., Bunte, R., Saha, S., Wang, J., Guo, C., He, W., and Kashina, A. (2010). Arginylation-dependent neural crest cell migration is essential for mouse development. PLoS Genet *6*, e1000878.

Kwon, Y.T., Kashina, A.S., Davydov, I.V., Hu, R.-G., An, J.Y., Seo, J.W., Du, F., and Varshavsky, A. (2002). An essential role of N-terminal arginylation in cardiovascular development. Science *297*, 96-99.

Matta-Camacho, E., Kozlov, G., Li, F.F., and Gehring, K. (2010). Structural basis of substrate recognition and specificity in the N-end rule pathway. Nat Struct Mol Biol *17*, 1182-1188.

Mogk, A., Schmidt, R., and Bukau, B. (2007). The N-end rule pathway of regulated proteolysis: prokaryotic and eukaryotic strategies. Trends Cell Biol *17*, 165-172.

Nillegoda, N.B., Theodoraki, M.A., Mandal, A.K., Mayo, K.J., Ren, H.Y., Sultana, R., Wu, K., Johnson, J., Cyr, D.M., and Caplan, A.J. (2010). Ubr1 and Ubr2 function in a quality control pathway for degradation of unfolded cytosolic proteins. Mol Biol Cell *21*, 2102-2116.

Nonaka, F., Kametani, F., Arai, T., Akiyama, H., and Hasegawa, M. (2009). Truncation and pathogenic mutations facilitate the formation of intracellular aggregates of TDP-43. Hum Mol Genet *18*, 3353-3364.

Pesiridis, G.S., Tripathy, K., Tanik, S., Trojanowski, J.Q., and Lee, V.M. (2011). A "two-hit" hypothesis for inclusion formation by carboxyl-terminal fragments of TDP-43 protein linked to RNA depletion and impaired microtubule-dependent transport. J Biol Chem *286*, 18845-18855.

Piatkov, K.I., Brower, C.S., and Varshavsky, A. (2012a). The N-end rule pathway counteracts cell death by destroying proapoptotic protein fragments. Proc Natl Acad Sci USA *109*, E1839-E1847.

Piatkov, K.I., Colnaghi, L., Bekes, M., Varshavsky, A., and Huang, T.T. (2012b). The auto generated fragment of the Usp1 deubiquitylase is a physiological substrate of the N-end rule pathway. Mol Cell *48*, 926-933.

Pop, C., and Salvesen, G.S. (2009). Human caspases: activation, specificity, and regulation. J Biol Chem *284*, 21777-21781.
Spires-Jones, T.L., Kopeikina, K.J., Koffie, R.M., de Calignon, A., and Hyman, B.T. (2011). Are tangles as toxic as they look? J Mol Neurosci *45*, 438-444.
Suzuki, T., and Varshavsky, A. (1999). Degradation signals in the lysine-asparagine sequence space. EMBO J *18*, 6017-6026.
Swerdlow, P.S., Finley, D., and Varshavsky, A. (1986). Enhancement of immunoblot sensitivity by heating of hydrated filters. Anal Biochem *156*, 147-153.
Tasaki, T.S., Sriram, S.M., Park, K.S., and Kwon, Y.T. (2012). The N-end rule pathway. Annu Rev Biochem *81*, 261-289.
Varshavsky, A. (2005). Ubiquitin fusion technique and related methods. Meth Enzymol *399*, 777-799.
Varshavsky, A. (2011). The N-end rule pathway and regulation by proteolysis. Prot Sci *20*, 1298-1345.
Varshavsky, A. (2012). Augmented generation of protein fragments during wakefulness as the molecular cause of sleep: a hypothesis. Prot Sci *21*, 1634-1661.
Wang, H., Piatkov, K.I., Brower, C.S., and Varshavsky, A. (2009). Glutamine-specific N-terminal amidase, a component of the N-end rule pathway. Mol Cell *34*, 686-695.
Wang, I.F., Chang, H.Y., Hou, S.C., Liou, G.G., Way, T.D., and Shen, C.K.J. (2012). The self interaction of native TDP-43 C terminus inhibits its degradation and contributes to early proteinopathies. Nat Commun *3*, 766.
Wang, J., Han, X., Saha, S., Xu, T., Rai, R., Zhang, F., Wolf, Y.I., Wolfson, A., Yates, J.R.r., and Kashina, A. (2011). Arginyltransferase is an ATP-independent self-regulating enzyme that forms distinct functional complexes in vivo. Chem Biol *18*, 121-130.
Zhang, F., Saha, S., Shabalina, S.A., and Kashina, A. (2010). Differential arginylation of actin isoforms is regulated by coding sequence-dependent degradation. Science *329*, 1534-1537.
Zilka, N., Kovacech, B., Barath, P., E., K., and Novák, M. (2012). The self-perpetuating tau truncation circle. Biochem Soc Trans *40*, 681-686.